Electronic Supplementary Material (ESI) for Journal of Materials Chemistry A.

Electronic Supplementary Material

Rational design of metal oxide hollow nanostructures decorated carbon nanosheets for superior lithium storage

Yanfeng Dong, Shaohong Liu, Yang Liu, Yongchao Tang, Ting Yang, Xuzhen Wang, Zhiyu Wang*, Zongbin Zhao* and Jieshan Qiu*

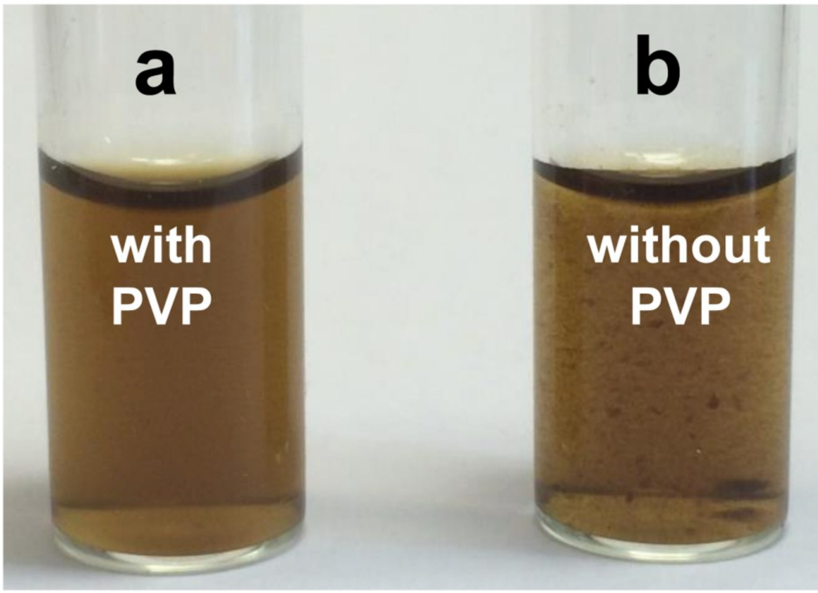

Fig.S1 Photos of $Fe(NO_3)_3$ (0.05 g) and GO (0.01 g) mixed solution (20 mL) with (a) or without (b) PVP (0.01 g).

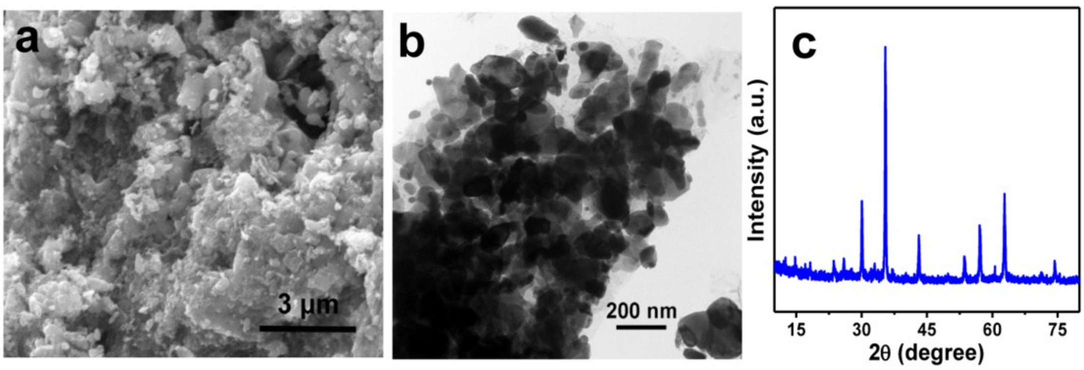

Fig.S2 SEM (a), TEM (b) images and XRD pattern (c) of Fe_2O_3/G.

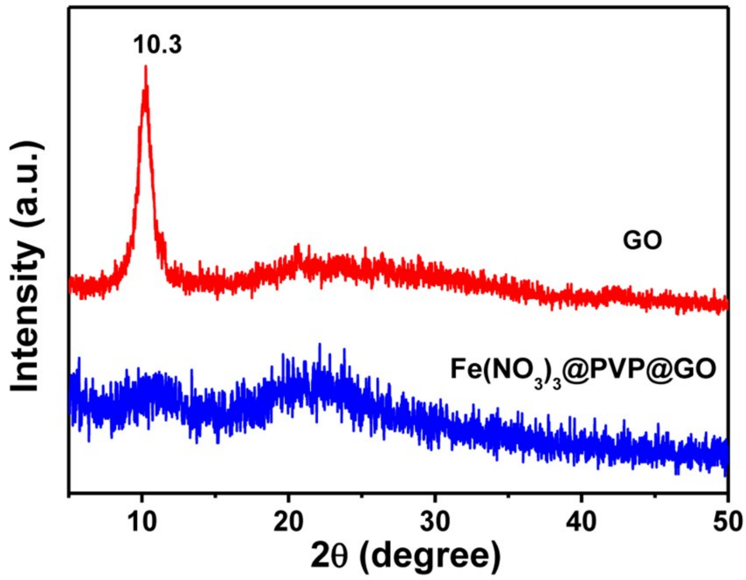

Fig.S3 XRD patterns of GO and $Fe(NO_3)_3$@PVP@GO.

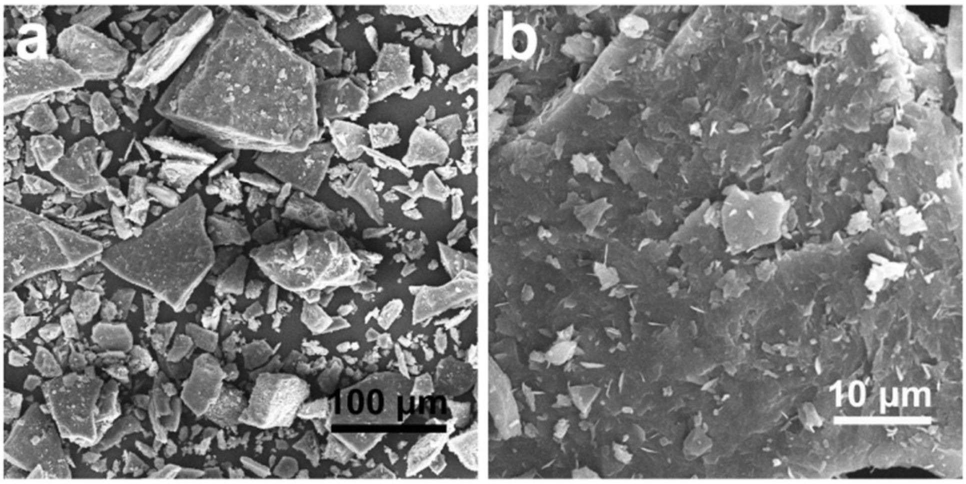

Fig.S4 (a) Low magnification SEM image of $Fe(NO_3)_3$@PVP@GO, suggesting the dense and bulk particles. (b) SEM image of a bulk $Fe(NO_3)_3$@PVP@GO particle, indicating the thick and multilayered nanostructures.

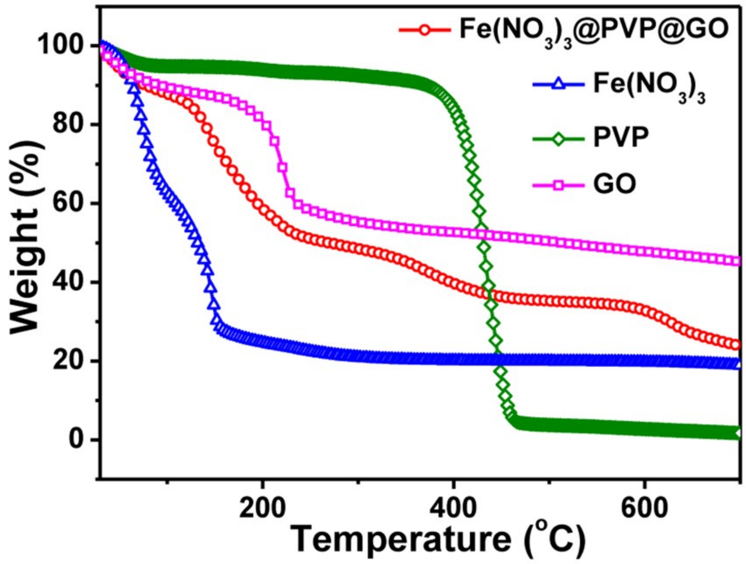

Fig.S5 Thermogravimetric analysis of GO, PVP, iron nitrate and $Fe(NO_3)_3$@PVP@GO in nitrogen atmosphere at 10 ^oC min^{-1} heating rate.

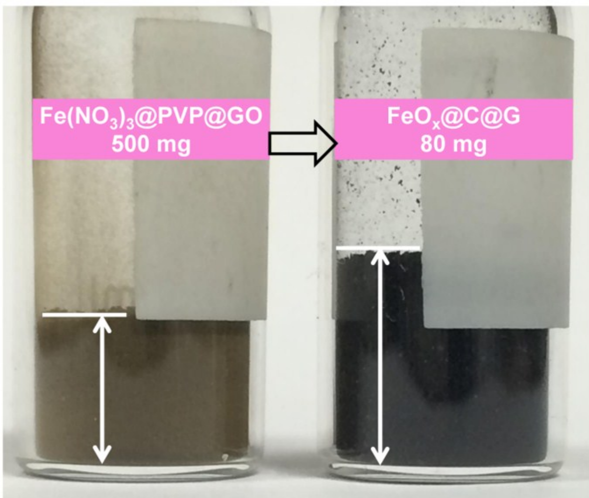

Fig.S6 Photo image (left) of 500 mg $Fe(NO_3)_3$@PVP@GO powder in a glass container, after carbonation process, the volume of the resulting 80 mg FeO_x@C@G exceeds that of $Fe(NO_3)_3$@PVP@GO (right).

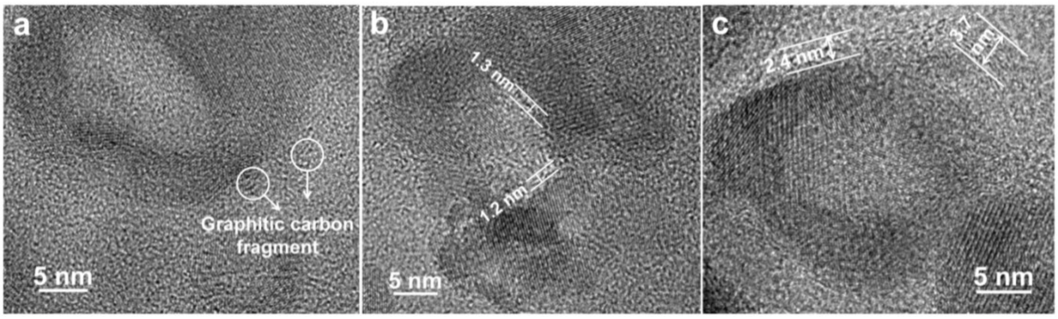

Fig.S7 HRTEM images of h-Fe_2O_3@C@G with 84 wt.% Fe_2O_3(a), 78 wt.% Fe_2O_3(b) and 70 wt.% Fe_2O_3(c).

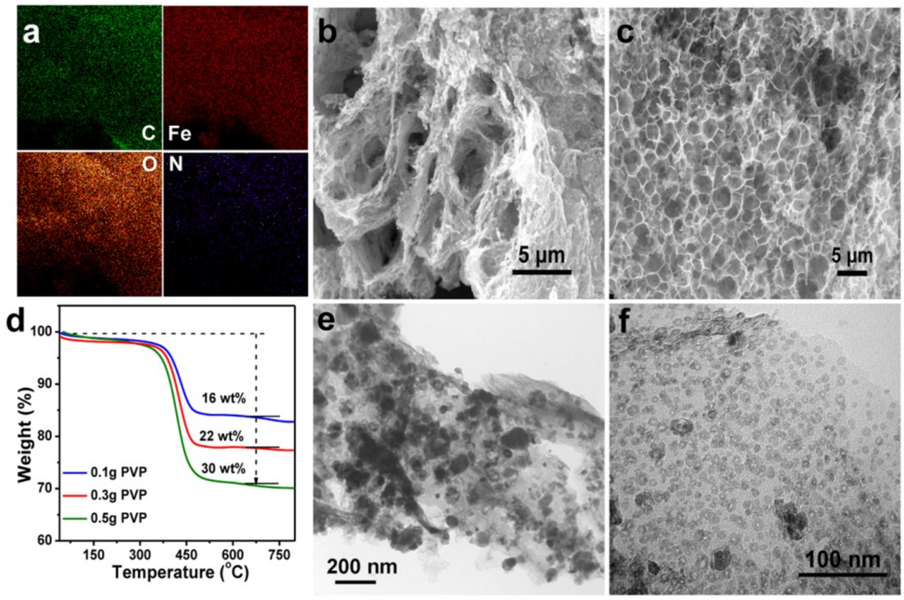

Fig.S8 (a) Elemental analysis of h-Fe_2O_3@C@G hybrids (with 0.3 g PVP dose), in which element C, N, Fe and O uniformly disperse in the observed zone; SEM image (b) and TEM image (e) of h-Fe_2O_3@C@G with 0.1 g PVP dose (corresponding to 84 wt.% Fe_2O_3); SEM image (c) and TEM image (f) of h-Fe_2O_3@C@G with 0.5 g PVP dosage (corresponding to 70 wt.% Fe_2O_3); (d) TGA analysis of h-Fe_2O_3@C@G hybrids with different Fe_2O_3 contenting, which are recorded under air atmosphere at 10 ^oC min^{-1}.

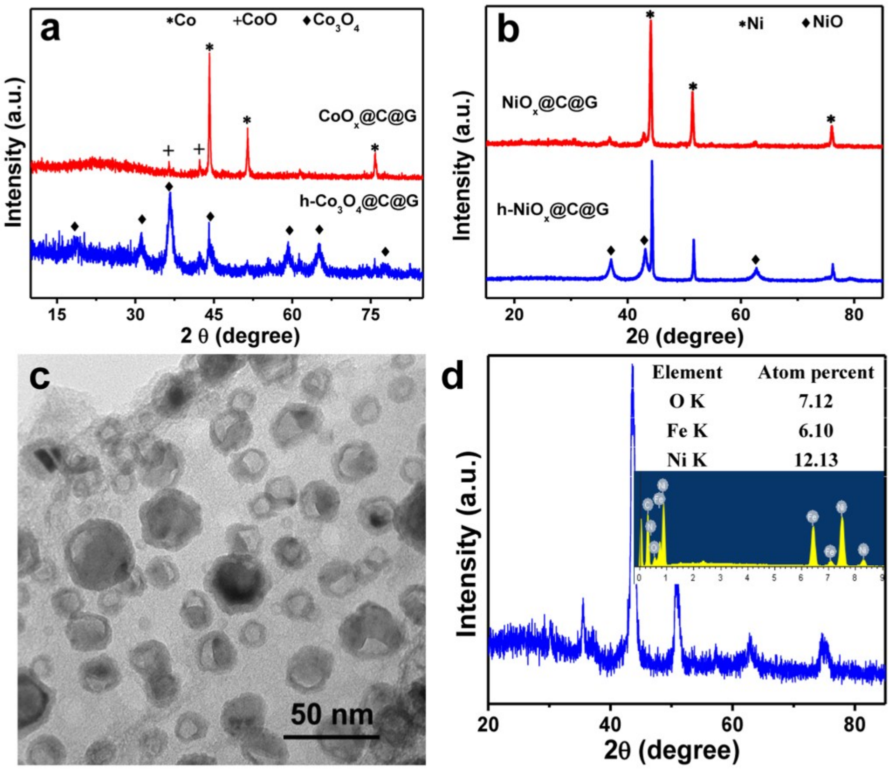

Fig.S9 (a) XRD patterns of CoO_x@C@G and h-Co_3O_4@C@G hybrids; (b) XRD patterns of NiO_x@C@G and h-NiO_x@C@G hybrids; (c) TEM image of h-$FeNiO_x$@C@G; (d) XRD pattern and element analysis (inset) of h-$FeNiO_x$@C@G hybrid.

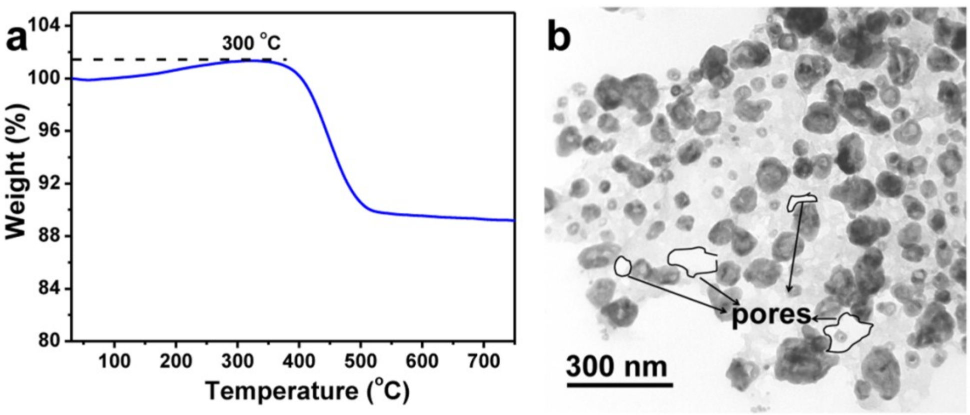

Fig.S10 (a) TGA analysis of $FeNiO_x$@C@G hybrid in air at the heating rate of 10 ^{o}C min^{-1}; (b) TEM image of h-$FeNiO_x$@C@G hybrid synthesized by air oxidation at 310 ^{o}C, in which many pores created by over oxidation of carbon could be found.

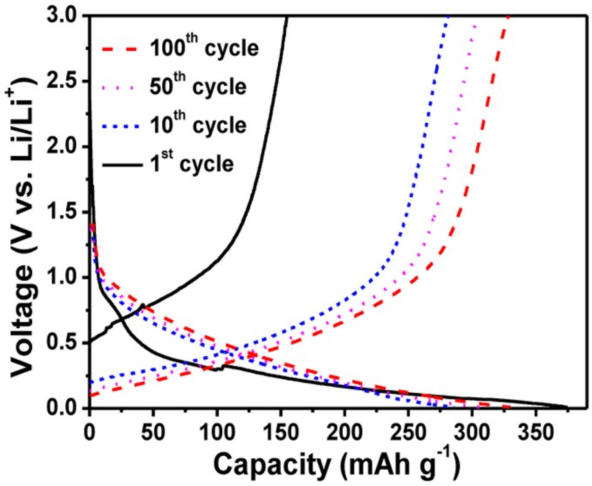

Fig.S11 Discharge/charge voltage profiles of G anode at 1A g^{-1}.

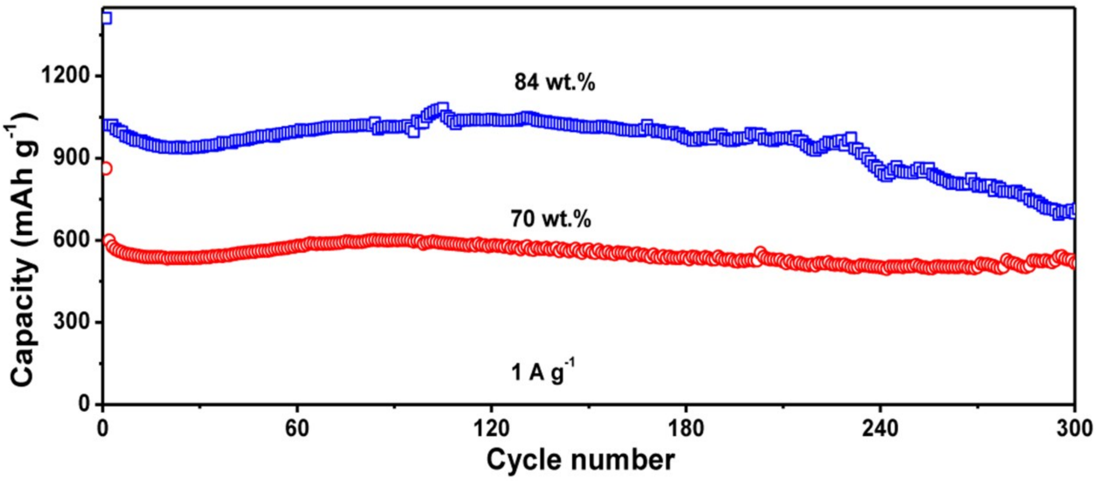

Fig.S12 Cycling stability of h-Fe_2O_3@C@G anodes with 84 wt.% Fe_2O_3 content and with 70 wt.% Fe_2O_3 content at 1 A g^{-1}.

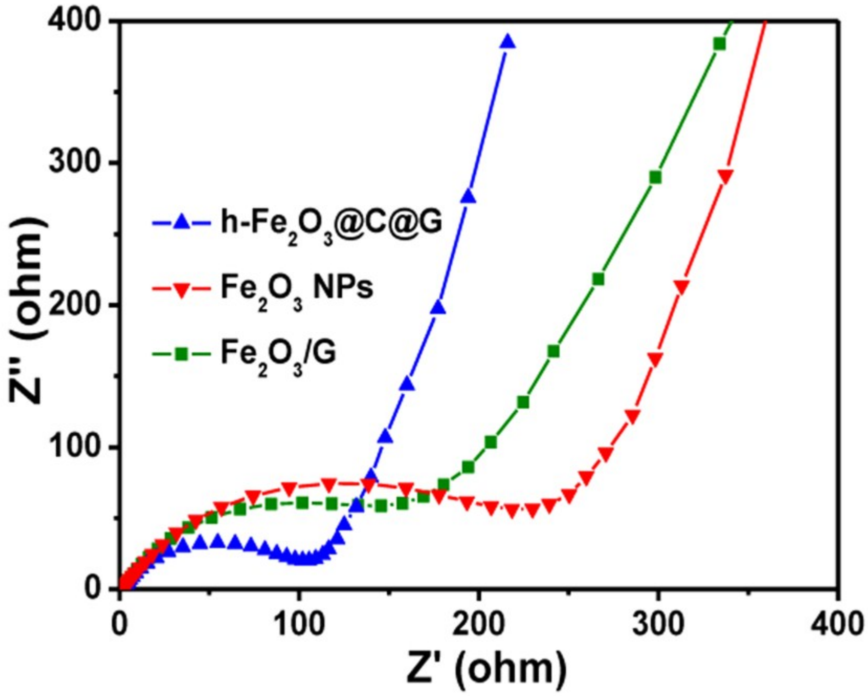

Fig.S13 Nyquist plots of Fe_2O_3 NPs, Fe_2O_3/G and h-Fe_2O_3@C@G anodes.

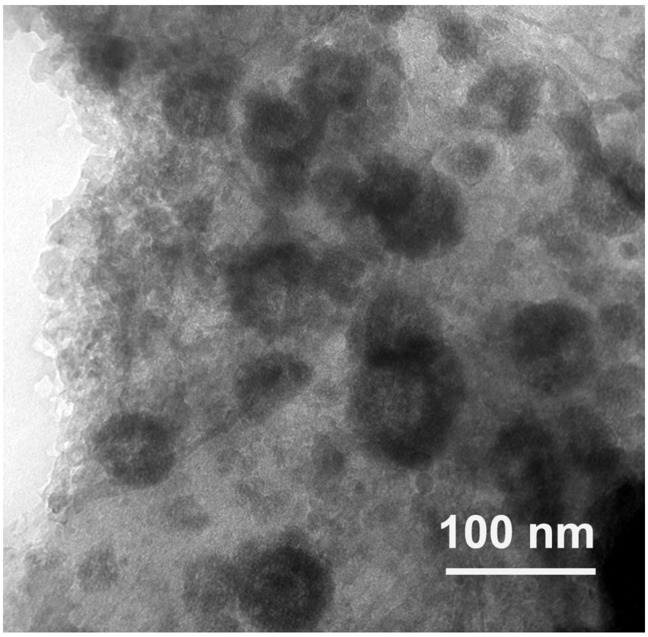

Fig.S14 TEM image of cycled h-Fe_2O_3@C@G anode.

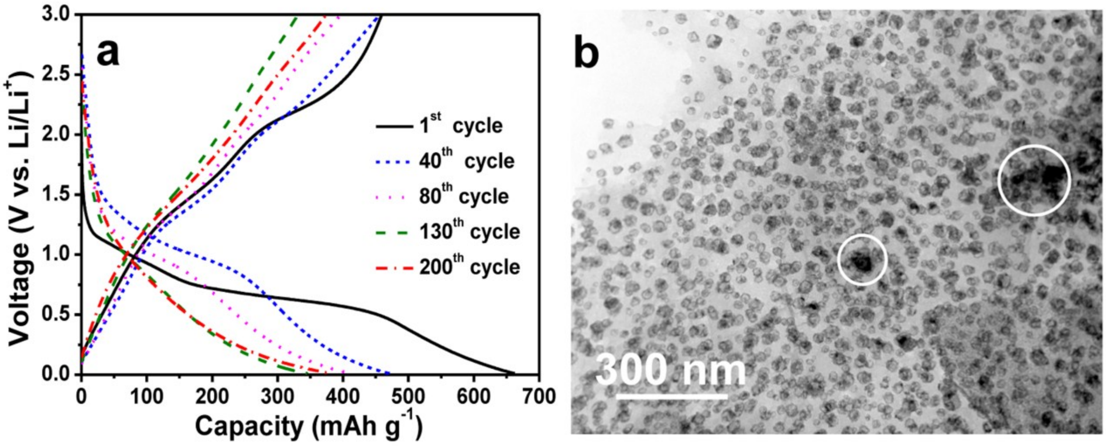

Fig.S15 (a) Discharge/charge voltage profiles of h-NiO_x@C@G anode, and (b) TEM image of h-NiO_x@C@G hybrid, in which few solid sphere or big particles could be found.

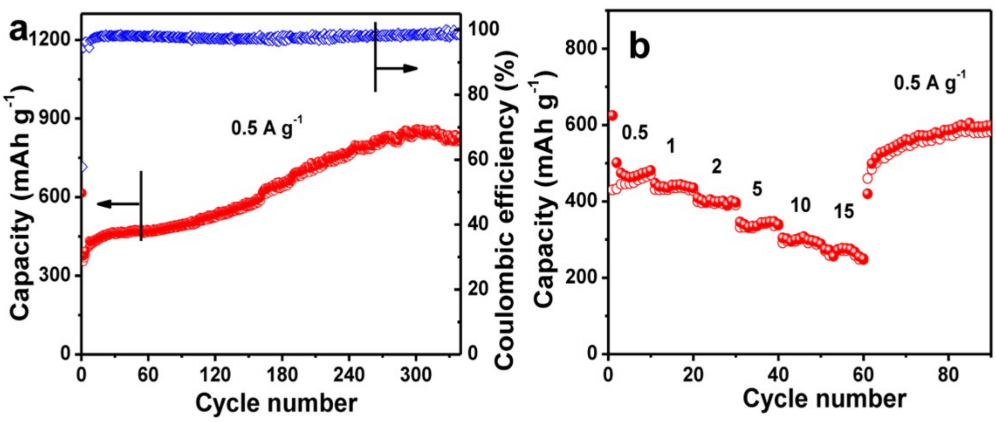

Fig.S16 Cycling stability (a) at 0.5 A g^{-1} and rate capability (b) of the h-$FeNiO_x$@C@G anode.

Table S1 A comparison of the electrochemical properties between h-Fe_2O_3@C@G anodes and other iron oxide-graphene electrodes

Active materials	Electrochemical properties	Reference
h-Fe_2O_3@C@G	**430-1163 mAh g^{-1} at 0.5-15 A g^{-1}, 724 mAh g^{-1} for 500 cycles at 5 A g^{-1}**	**This work**
3D Fe_2O_3 /N-doped graphene	420-1140 mAh g^{-1} at 0.2-6.0 A g^{-1}, 11200 mAh g^{-1} for 500 cycles at 0.50 A g^{-1}	Ref [1]
Bubble-nanorod structured Fe_2O_3/C nanofibers	491-913 mAh g^{-1} at 0.5-5 A g^{-1}, 824 mAh g^{-1} for 300 cycles at 1 A g^{-1}	Ref [2]
Yolk-shell FeO_x@C structure	370-843 mAh g^{-1} at 0.2-4 A g^{-1}	Ref [3]
Iron oxide-rGO	~500-1050 mAh g^{-1} at 0.1-1.6 A g^{-1}	Ref [4]
Porous iron oxide ribbons -graphene	615 mAh g^{-1} at 1.86 A g^{-1} 1046 mAh g^{-1} for 130 cycles at 0.074 A g^{-1}	Ref [5]
α-Fe_2O_3/graphene	615 mAh g^{-1} at 5 A g^{-1} 1046 mAh g^{-1} for 130 cycles at 0.074 A g^{-1}	Ref [6]
Fe_3O_4/CN_x/rGO	450-1110 mAh g^{-1} at 0.1-10 A g^{-1}, 590 mAh g^{-1} for 500 cycles at 5 A g^{-1}	Ref [7]
Hollow Fe_3O_4@graphene	420-900 mAh g^{-1} at 0.2- 2 A g^{-1}, 940 mAh g^{-1} for 50 cycles at 0.2 A g^{-1}	Ref [8]
Fe_3O_4/CNTs @graphene	150-850 mAh g^{-1} at 0.15-2.4 A g^{-1}, 680 mAh g^{-1} for 100 cycles at 0.2 A g^{-1}	Ref [9]
2D G@Fe_3O_4@C	550-900 mAh g^{-1} at 0.2-0.5 A g^{-1}	Ref [10]
Fe_3O_4/graphene	629-913 mAh g^{-1} at 0.1-2 A g^{-1}	Ref [11]
Fe_3O_4@graphene	410-740 mAh g^{-1} at 0.3-1.0 A g g^{-1}, 1048 mAh g^{-1} for 90 cycles at 0.1 A g^{-1}	Ref [12]

Referenece

[1] R. Wang, C. Xu, J. Sun, L. Gao, *Sci. Rep.* **2014**, *4*, 7171.

[2] J. S. Cho, Y. J. Hong, Y. C. Kang, *ACS Nano* **2015**, *9*, 4026.

[3] H. Zhang, L. Zhou, O. Noonan, D. J. Martin, A. K. Whittaker, C. Yu, *Adv. Funct. Mater.* **2014**, *24*, 4337.
[4] S.-H. Yu, D. E. Conte, S. Baek, D.-C. Lee, S.-K. Park, K. J. Lee, Y. Piao, Y.-E. Sung, N. Pinna, *Adv. Funct. Mater.* **2013**, *23*, 4293.
[5] S. Yang, Y. Sun, L. Chen, Y. Hernandez, X. Feng, K. Müllen, *Sci. Rep.* **2012**, *2*, 427.
[6] B. Jang, O. B. Chae, S.-K. Park, J. Ha, S. M. Oh, H. B. Na, Y. Piao, *J. Mater. Chem. A* **2013**, *1*, 15442.
[7] S. Liu, Y. Dong, C. Zhao, Z. Zhao, C. Yu, Z. Wang, J. Qiu, *Nano Energy* **2015**, *12*, 578.
[8] R. Wang, C. Xu, J. Sun, L. Gao, C. Lin, *J. Mater. Chem. A* **2013**, *1*, 1794.
[9] S. Yang, C. Cao, G. Li, Y. Sun, P. Huang, F. Wei, W. Song, *Nano Res.* **2015**, *8*, 1339.
[10] Y. Su, S. Li, D. Wu, F. Zhang, H. Liang, P. Gao, C. Cheng, X. Feng, *ACS Nano* **2012**, *6*, 8349.
[11] B. Zhao, Y. Zheng, F. Ye, X. Deng, X. Xu, M. Liu, Z. Shao, *ACS Appl. Mater. Interfaces* **2015**, *7*, 14446.
[12] P. Lian, X. Zhu, H. Xiang, Z. Li, W. Yang, H. Wang, *Electrochim. Acta* **2010**, *56*, 834.